Karson, J.A., Cannat, M., Miller, D.J., and Elthon, D. (Eds.), 1997
Proceedings of the Ocean Drilling Program, Scientific Results, Vol. 153

32. *DATA REPORT:* REORIENTATION OF STRUCTURAL FEATURES AT SITES 920 TO 924 USING REMANENT MAGNETIZATION AND MAGNETIC CHARACTERISTICS[1]

Stephen D. Hurst,[2] Jeff S. Gee,[3] and Róisín M. Lawrence[2]

ABSTRACT

Drilling at Ocean Drilling Program Sites 920 to 924 recovered core with a diverse set of pervasive structural elements. Site 920 recovered predominantly peridotitic rocks that display an early crystal-plastic fabric overprinted by at least five generations of veins. Sites 921 to 924 recovered gabbros that contain magmatic and metamorphic foliations and lineations developed to varying intensities throughout. Brittle features in the gabbro core include cataclastic zones, faults, and several generations of veins. The characteristic magnetization direction was used to estimate the in situ orientation of structural features within the core. Although significant uncertainty is associated with the unknown effects of anisotropy and tectonic rotations on the remanent declinations, the corrected attitudes of the dominant foliations at Site 920 dip gently east-northeast, parallel to other observations of seafloor structures in the area. Other vein generations and structural features in the rocks do not have a consistent orientation with respect to each other or a consistent variation with core depth. Sites 921–924 were drilled into a section of mostly gabbroic rocks that typically have complicated magnetic properties, with several remanence components identifiable during demagnetization. Reorientation of the gabbro cores is less certain because of the complexity of the remanent magnetization components, however, many structures in the gabbro from Hole 923A also seem to have gentle dips to the northeast after such a reorientation.

INTRODUCTION

Ocean Drilling Program (ODP) Sites 920 to 924 are located on the median valley wall of the Mid-Atlantic Ridge near the Kane Transform Zone (MARK area; Fig. 1). The sites are located about 10 km west of the neovolcanic ridge in the center of the valley. The holes were drilled into serpentinized peridotite (Site 920) and gabbro (Sites 921–924) exposures thought to represent upper mantle and middle to lower oceanic crust. The most prevalent theory for their exposure entails significant faulting and tectonic extension (Karson and Dick, 1983; Karson, 1990; Karson and Lawrence, this volume). The age of these rocks is 0.6 to 0.9 Ma, as determined using a 1.3 cm/yr half-spreading rate (Schultz et al., 1988; corrected for 0.78 Ma as the age of the Brunhes/Matuyama boundary). The presence of reversed polarity magnetizations at Sites 921–923 indicates a minimum age of 0.78 Ma for these lower crustal gabbros. The uniform normal polarity of the peridotites from Site 920 is consistent with acquisition of the remanent magnetization during the last 0.78 m.y. However, because of the likely role of low-angle extensional faulting in exposing the rocks, the actual age of the rocks remains uncertain. (Bonatti, 1976; Karson and Dick, 1983; Karson, 1990; Cannat, 1993; Cannat et al., 1995). For the peridotite samples, the acquisition of main magnetic remanence likely occurred during serpentinization, although a later thermal event or even the acquisition of a recent viscous remanence is possible. The timing of serpentinization of the peridotites is unknown.

Approximately 325 m of serpentinized peridotites with subsidiary gabbro and diabase intervals was drilled at Site 920 in two holes (Holes 920B and 920D), ~50 m apart. Rocks with very similar composition, structure, and mesoscopic fabric were recovered. In general, the dominant lithology is serpentinized harzburgite, which contains a pervasive mesoscopic foliation defined by elongate relict orthopyroxene grains and subparallel, white, serpentine veins. In much of the core, this foliation has a dip of about 30°. Dunitic intervals generally show fewer white serpentine veins, but commonly show a few elongate relict orthopyroxenes that define the early plastic fabric (Cannat, Karson, Miller, et al., 1995; Ceuleneer and Cannat, this volume). The vast majority of peridotite samples have positive characteristic remanent inclinations in the range 25°– 45° (Fig. 2), suggesting magnetization during a single normal polarity interval. The main carrier of the magnetization is magnetite, randomly interspersed within the mesh-textured serpentine and aligned along the edges of serpentine veins (Lawrence et al., this volume).

Four sites (Sites 921–924) were drilled in gabbro exposures to the north of Site 920, at approximately the same distance from the center of the median valley as Site 920 (Fig. 1). All four sites are located within a radius of ~2 km. Two holes (Holes 921A and 923A) were drilled to depths of 80 m with an average recovery of 50%. The remaining gabbro holes were only drilled to depths of 40 m or less and had poorer recovery (Cannat, Karson, Miller, et al., 1995).

The gabbros from Sites 921 to 924 include olivine gabbros, metagabbronorites, troctolites, Fe-Ti oxide gabbros, and minor volumes of other gabbroic lithology. About 40% of the gabbros shows evidence of plastic deformation (Shipboard Scientific Party, 1995c, 1995d; Gaggero and Luciano, this volume). The plastic deformation ranges from a subtle foliation and lineation with evident recrystallization of plagioclase in hand specimen to strongly deformed mylonitic zones tens of centimeters thick. A significant proportion of the gabbros (~20%) consists of lineated and foliated rocks that have lamellar-twinned plagioclase crystals with no undulose extinction or irregular twins indicative of plastic deformation (Shipboard Scientific Party, 1995c, 1995d). The remainder of the core shows no mesoscopic evidence of any penetrative foliation or lineation.

The demagnetization behavior of the gabbro samples is typically much more complex than that of the peridotites, with two and occasionally three or more magnetization components identified (fig. 84 in Shipboard Scientific Party, 1995c). These components have both positive and negative inclinations, indicating that the acquisition of magnetization spanned two or more polarity intervals. Alteration in

[1]Karson, J.A., Cannat, M., Miller, D.J., and Elthon, D. (Eds.), 1997. *Proc. ODP, Sci. Results,* 153: College Station, TX (Ocean Drilling Program).

[2]Department of Geology, Duke University, Durham, NC 27708, U.S.A. steve@geo.duke.edu

[3]Geosciences Research Division, Scripps Institution of Oceanography, La Jolla, CA 92014, U.S.A.

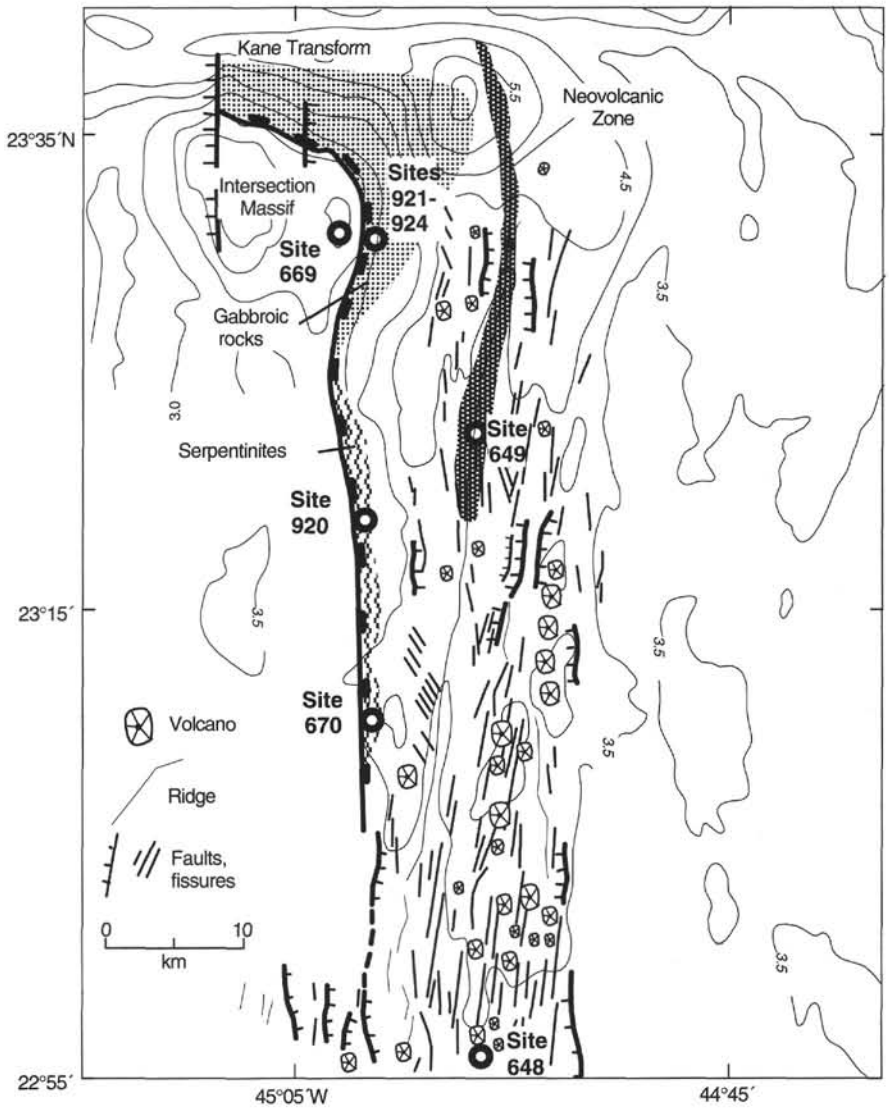

Figure 1. Generalized geologic map of the MARK area, Mid-Atlantic Ridge at 22°–24°N. Contours in km below sea level.

the gabbros may form a spurious, well-defined characteristic magnetization component such as that seen in some of the gabbro samples (Gee et al., this volume). However, some gabbro samples show a single characteristic remanence with an inclination similar to the expected geocentric axial dipole in the area (41°).

REORIENTATION PROCEDURE

During drilling operations on Leg 153, each piece of core was free to rotate about the vertical axis within the core barrel. No downhole logging was done in any of the holes drilled, therefore the only conceivable means of reorienting the core is using the paleomagnetic demagnetization data (e.g., Cannat and Pariso, 1991). The inclination and declination of the stable remanent magnetic vector were measured in 202 peridotite and 329 gabbro samples (Shipboard Scientific Party, 1995b, 1995d; Gee et al., this volume). Because of the consistent inclination of the characteristic magnetization component in the peridotites, the paleomagnetic vector in each piece of peridotite might, to first order, be inferred to point in the same direction before drilling. The reorientation procedure discussed here applies mainly to peridotite samples (Site 920). However, a small number of structural features from one gabbro site (Hole 923A) are also reoriented using the same procedure.

A total of 153 core pieces or subpieces from Site 920, having either planar or linear structural features measured during shipboard core description, was reoriented using characteristic stable remanence data determined from principle component analysis (Kirschvink, 1980). All the reoriented structural data, including the characteristic declination for Holes 920B and 920D, are reported here, including the data from the 119 core pieces with shipboard paleomagnetic measurements (Tables 1, 2). Each reoriented structural feature was in the same piece or subpiece as the paleomagnetic measurement, generally within 15 cm. All of the original measurements were made relative to the ODP core coordinate system (Fig. 3)(Shipboard Scientific Party, 1995a). The shipboard analysis and subsequent shore-based work verified that almost all serpentinized peridotite samples contain a univectorial characteristic magnetization with an average inclination of 35.2° ± 1° (N = 202, the uncertainty is the half angle of the asymmetric 95% confidence interval, calculated using the inclination-only method of McFadden and Reid [1982]). This average inclination is somewhat less than the inclination (41°) expected for a geocentric axial dipole (GAD) at this site. There are many possible reasons for this discrepancy between the measured average characteristic inclination and the inclination predicted from a GAD model. One explanation may be that secular variation is inadequately averaged. Because the sole magnetic carrier in the peridotites is magnetite that formed in mesh-textured bulk serpentine as well as

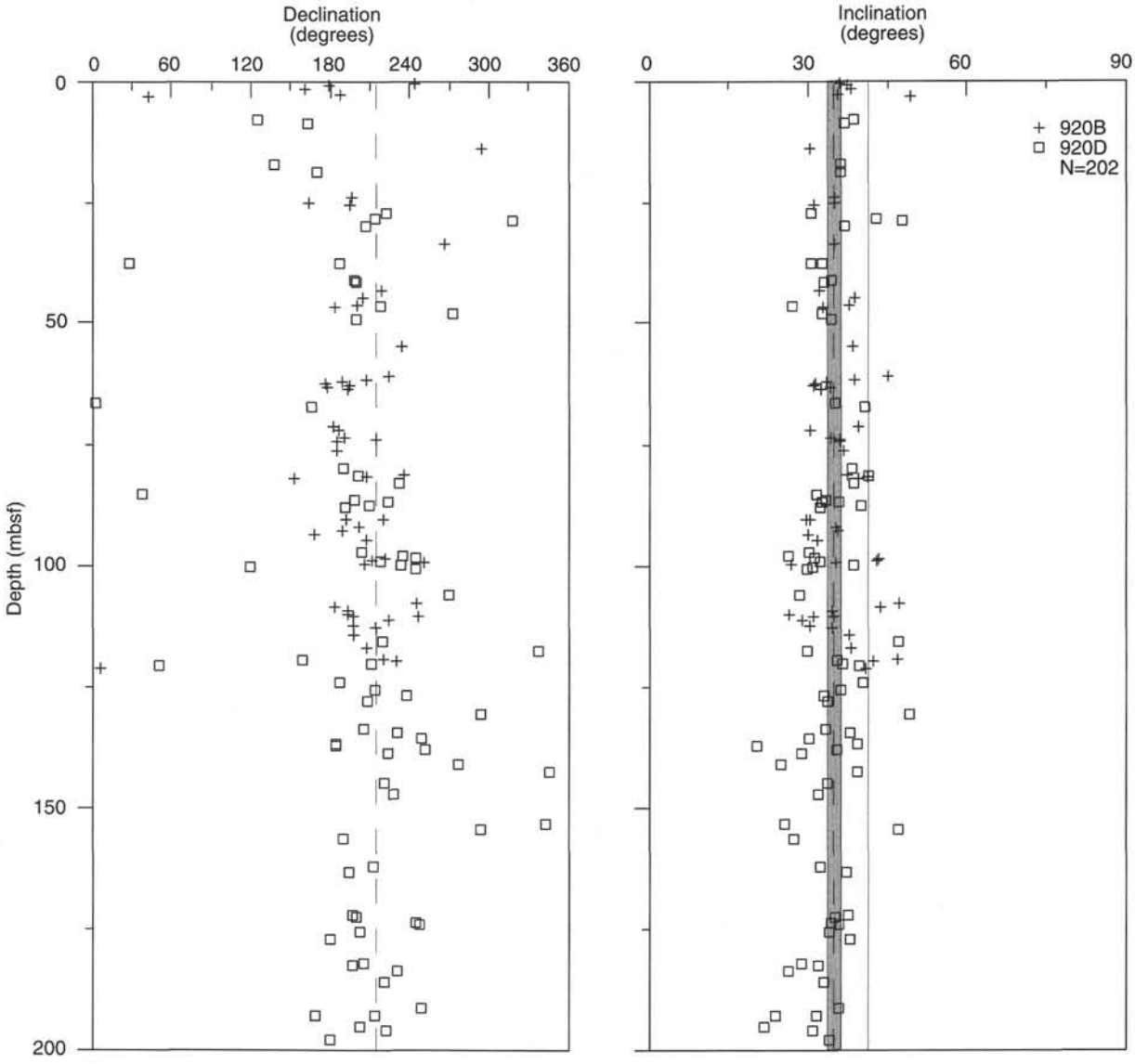

Figure 2. Characteristic remanent declination and inclination vs. depth for 202 discrete minicore samples taken from core from Holes 920B and 920D. Dashed vertical lines show the average value for the combined measurements. The gray box on the inclination plot defines the asymmetric 95% confidence limits for the mean of the measurements (McFadden and Reid, 1982). The solid vertical line is the expected inclination for a geocentric axial dipole at this latitude (41°).

along crosscutting serpentine veins, the characteristic remanence must have been acquired during or after serpentinization. There are several generations of veins with consistent crosscutting relationships as well as serpentinized remnants of pyroxene and olivine throughout the serpentinized peridotite core. The serpentinization of olivine, pyroxene, and the creation of a succession of serpentine vein sets probably took sufficient time to average secular variation, making inadequate averaging of secular variation an unsatisfactory explanation.

Another possible reason for the discrepancy between the measured inclinations and the expected inclination may be the substantial degree of anisotropy in the magnetic susceptibility (AMS). The AMS is high (average $K_1/K_3 = 1.19$) in all the peridotite samples measured (N = 202) (Table 3; Shipboard Scientific Party, 1995b; Lawrence et al., this volume). High degrees of anisotropy of susceptibility, if also indicative of the anisotropy of the remanence-carrying grains, may possibly result in a deflection of remanence acquisition by up to 3° per 5% anisotropy (Stacey and Banerjee, 1974). The actual amount of deflection depends upon the angular relationship between the applied field and the orientation of the susceptibility principle axes. Upon reorientation of the characteristic declinations of the peridotites to 0°, the maximum axis (K_1) of the susceptibility ellipsoid is directed to 0° azimuth with a very shallow plunge, and the minimum axis (K_3) is directed west with approximately a 30° plunge (Fig. 4). Therefore the direction of K_1 is typically 25°–30° towards the horizontal from the characteristic magnetization direction. Given the known tectonism at this portion of the Mid-Atlantic Ridge and the expectation that serpentinized peridotites are a lower crustal rock type, another cause of the inclination discrepancy may be rotation of the magnetization by postserpentinization deformation. The majority of faults in the area trend 0°–10°; parallel to the axial valley. Assuming that a rotation about a horizontal, north-south axis caused the characteristic inclination to decrease, then a rotation of ~30° would be needed to change the inclination from 41° to the observed 35° (Fig. 5 and Shipboard Scientific Party, 1995b). This rotation would also cause the declination to change from 0° to ± 23°. Rotations about other horizontal axes would need correspondingly less rotation to change the inclination, and would also have proportionally less of an effect on

Table 1. Reorientation data for samples from Hole 920B.

Core, section	Piece	Char. declin. (°) (uncorr.)	Feature	Strike, dip (°) (uncorr.)	Strike, dip (°) (corr.)
1W-1	6	244	Pf	180, 40	296, 40
1W-1	6	244	V3	290, 79	46, 79
1W-2	6	159	V0	211, 66	52, 66
1W-2	1	181	V2a	36, 51	215, 51
1W-2	6	159	V2a	186, 40	27, 40
1W-3	4	188	Pf	149, 48	321, 48
1W-3	6	43	Pf	56, 46	13, 46
1W-3	4	188	V1	210, 48	22, 48
1W-3	6	43	V1	42, 43	359, 43
1W-3	6	43	V2	132, 15	89, 15
1W-3	4	188	V2	140, 76	312, 76
1W-3	4	188	V3	135, 60	307, 60
2R-1	2	294	V2	338, 40	44, 40
2R-1	2	294	V3	343, 72	49, 72
3R-1	5	196	Af	175, 25	339, 25
3R-1	5	196	Pf	175, 20	339, 20
3R-1	5	196	V2	175, 25	339, 25
3R-1	5	196	V3	102, 90	266, 90
3R-2	10	194	Af	170, 45	336, 45
3R-2	4	164	Pf	169, 48	5, 48
3R-2	10	194	Pf	162, 46	328, 46
3R-2	4	164	V1	168, 82	4, 82
3R-2	10	194	V1	172, 27	338, 27
3R-2	4	164	V2	177, 38	13, 38
3R-2	10	194	V2	170, 45	336, 45
4R-1	7	266	Af	180, 25	274, 25
4R-1	7	266	Pf	180, 25	274, 25
4R-1	7	266	V2	180, 25	274, 25
5R-2	10	205	Af	180, 40	335, 40
5R-2	10	205	Pf	180, 40	335, 40
5R-2	10	205	V2	180, 37	335, 37
6R-3	2	234	Pf	120, 59	246, 59
6R-3	2	234	V2	147, 51	273, 51
6R-3	2	234	V3	282, 18	48, 18
7R-1	3B	224	Af	257, 77	33, 77
7R-1	4A	207	Af	222, 65	15, 65
7R-1	5B	189	Af	142, 43	313, 43
7R-1	3A	224	CL	230, 54	6, 54
7R-1	5A	189	CL	144, 30	315, 30
7R-1	3E	224	Pf	165, 47	301, 47
7R-1	4A	207	Pf	194, 60	347, 60
7R-1	5B	189	Pf	209, 42	20, 42
7R-1	4B	207	V0	31, 49	184, 49
7R-1	3B	224	V2	257, 77	33, 77
7R-1	4A	207	V2	231, 63	24, 63
7R-1	4B	207	V2	189, 77	342, 77
7R-1	5B	189	V2	142, 43	313, 43
7R-1	3B	224	V3	135, 58	271, 58
7R-1	4A	207	V3	223, 78	16, 78
7R-1	5B	189	V3	201, 90	12, 90
7R-2	1B	176	Af	145, 57	329, 57
7R-2	4A	195	Af	222, 50	27, 50
7R-2	8	178	Af	190, 50	12, 50
7R-2	1B	176	MV	50, 54	234, 54
7R-2	1B	176	Pf	143, 56	327, 56
7R-2	4A	195	Pf	219, 54	24, 54
7R-2	8	178	Pf	165, 35	347, 35
7R-2	1B	176	V2	211, 44	35, 44
7R-2	4A	195	V2	222, 50	27, 50
7R-2	8	178	V2	190, 50	12, 50
7R-2	1B	176	V3	148, 45	332, 45
7R-3	1	193	Af	190, 30	357, 30
7R-3	1	193	Pf	190, 30	357, 30
7R-3	1	193	V1	331, 42	138, 42
7R-3	1	193	V2	190, 30	357, 30
8R-1	12	182	Pf	190, 20	8, 20
8R-1	12	182	V2	189, 33	7, 33
8R-2	6	187	Af	174, 38	347, 38
8R-2	6	187	V0	79, 15	252, 15
8R-2	6	187	V2	169, 36	342, 36
8R-3	11	214	Af	180, 40	326, 40
8R-3	11	214	Pf	180, 40	326, 40
8R-3	7	190	V0	190, 32	0, 32
8R-3	11	214	V0	198, 32	344, 32
8R-3	7	190	V2	184, 42	354, 42
8R-3	11	214	V2	180, 40	326, 40
8R-4	2	185	Pf	169, 25	344, 25
8R-4	2	185	V0a	15, 61	190, 61
8R-4	2	185	V2	187, 34	2, 34
8R-5	5	185	V0	202, 33	17, 33
8R-5	5	185	V2	192, 31	7, 31
9R-2	5	152	Af	102, 70	310, 70
9R-2	5	152	Pf	102, 70	310, 70
9R-2	5	152	V1	102, 70	310, 70
9R-2	4	207	V1a	195, 82	348, 82
9R-2	4	207	V1b	229, 11	22, 11
9R-2	1	236	V2	189, 44	313, 44
9R-2	3	236	V2	189, 44	313, 44
9R-2	4	207	V2	180, 15	333, 15
9R-2	5	152	V2	230, 66	78, 66
9R-2	5	152	V3	184, 77	32, 77
10R-2	1	192	Af	153, 27	321, 27
10R-2	2	220	Af	205, 43	345, 43
10R-2	2	220	Pf	205, 43	345, 43
10R-2	1	192	V2	153, 27	321, 27
10R-2	2	220	V2	205, 43	345, 43
10R-2	2	220	V3	200, 81	340, 81
10R-3	5	202	Af	180, 40	338, 40
10R-3	8	189	Af	180, 35	351, 35
10R-3	5	202	Pf	180, 40	338, 40
10R-3	8	189	Pf	180, 35	351, 35
10R-3	8	189	V1	180, 35	351, 35
10R-3	8	189	V2	180, 70	351, 70
10R-3	5	202	V2a	180, 55	338, 55
10R-3	8	189	V3	180, 90	351, 90
10R-4	2	168	Af	188, 45	20, 45
10R-4	2	168	Pf	188, 45	20, 45
10R-4	2	168	V2	188, 45	20, 45
10R-5	1	206	Pf	191, 44	345, 44
10R-5	1	206	V2	180, 40	334, 40
11R-1	1	425	1MV	168, 32	277, 32
11R-1	2	222	Pf	190, 28	328, 28
11R-1	8	212	Pf	155, 32	303, 32
11R-1	14	251	Pf	168, 32	277, 32
11R-1	2	222	V2	190, 28	328, 28
11R-1	8	212	V2	155, 32	303, 32
11R-1	2	222	V3b	218, 54	356, 54
11R-2	1	206	Af	180, 39	334, 39
11R-2	1	206	Pf	180, 39	334, 39
11R-2	1	206	V2	180, 39	334, 39
12R-1	2	246	Af	224, 53	338, 53
12R-1	3	183	Af	160, 20	337, 20
12R-1	3	183	MV	161, 26	338, 26
12R-1	2	246	Pf	177, 37	291, 37
12R-1	3	183	Pf	167, 33	344, 33
12R-1	2	246	V0a	303, 34	57, 34
12R-1	2	246	V0b	265, 31	19, 31
12R-1	2	246	V2	183, 32	297, 32
12R-1	3	183	V2	160, 20	337, 20
12R-1	2	246	V3	127, 74	241, 74
12R-1	3	183	V3	241, 76	58, 76
12R-2	4	194	Af	173, 42	339, 42
12R-2	5	193	Af	167, 55	334, 55
12R-2	6	247	Af	15, 34	128, 34
12R-2	4	194	CL1	170, 16	336, 16
12R-2	4	194	CL2	232, 52	38, 52
12R-2	6	247	F1	284, 33	37, 33
12R-2	6	247	F1	L:32/310	L:32/197
12R-2	6	247	F2	277, 68	30, 68
12R-2	6	247	F2	L:42/302	L:42/189
12R-2	5	193	Pf	158, 5	325, 5
12R-2	4	194	V1	255, 26	61, 26
12R-2	6	247	V1	33, 57	146, 57
12R-2	4	194	V2	173, 42	339, 42
12R-2	5	193	V2	167, 55	334, 55
12R-2	6	247	V2	13, 55	126, 55
12R-3	8	224	Af	192, 43	328, 43
12R-3	3	197	V2	184, 68	347, 68
12R-3	8	224	V2	192, 43	328, 43
12R-4	4	197	V2	173, 59	336, 59
12R-5	1A	214	Af	129, 64	275, 64
12R-5	1A	214	V2	129, 64	275, 64
12R-5	1B	214	V3b	L:42/270	L:42/124
12R-6	1	197	Af1	176, 37	339, 37
12R-6	1	197	Af2	152, 28	315, 28
12R-6	1	197	MV	245, 48	48, 48
12R-6	1	197	MV	138, 31	301, 31
12R-6	1	197	Pf	162, 40	325, 40
12R-6	1	197	V2	176, 37	339, 37
13R-1	2	208	Af	140, 36	292, 36
13R-1	2	208	Pf	140, 36	292, 36
13R-1	2	208	V1	270, 18	62, 18
13R-1	2	208	V2	140, 36	292, 36
13R-2	7	220	Af	180, 28	320, 28
13R-3	1A	230	Af	150, 40	280, 40
13R-3	1A	230	Pf	170, 42	300, 42
13R-3	1A	230	V1	15, 71	145, 71
13R-3	1A	230	V2	150, 40	280, 40
13R-4	3	5.7	D1	206, 72	200, 72
13R-4	3	5.7	Pf	175, 70	169, 70

Notes: The correction factor is equal to 360° – D (the uncorrected stable remanent declination). Therefore the corrected orientations are in the system where north is parallel to the remanent declination. Char. declin. = characteristic declination, uncorr. = uncorrected, corr. = corrected. Feature abbreviations are described in Shipboard Scientific Party (1995a) and in other portions of this volume (Dilek, Coulton, et al., this volume).

Table 2. Reorientation data for samples from Hole 920D.

Core, section	Piece	Char. declin. (°) (uncorr.)	Feature	Strike, dip (°) (uncorr.)	Strike, dip (°) (corr.)
2R-1	4	126	V3	170, 36	44, 36
2R-1	4	126	V1	318, 67	192, 67
2R-1	4	126	V4	125, 47	359, 47
2R-1	13	164	V0	223, 17	59, 17
2R-1	13	164	Pf	132, 67	328, 67
3R-1	3	138	Af	165, 45	27, 45
3R-1	3	138	Pf	165, 45	27, 45
3R-1	3	138	V2	165, 45	27, 45
3R-1	3	138	V3	350, 58	212, 58
3R-2	4	171	Af	251, 15	80, 15
3R-2	4	171	Pf	251, 15	80, 15
3R-2	4	171	V2	251, 15	80, 15
3R-2	4	171	V3	81, 50	270, 50
4R-1	5	223	V3	75, 35	212, 35
4R-1	5	223	Af	180, 25	317, 25
4R-1	5	223	Pf	180, 25	317, 25
4R-1	5	223	V2	180, 25	317, 25
4R-2	3	214	V2	134, 30	280, 30
4R-2	3	214	V2	178, 22	324, 22
4R-2	6	318	V2	235, 31	277, 31
4R-3	5	207	V3	112, 13	265, 13
4R-3	5	207	V2	142, 37	295, 37
5R-1	10	29	Af	168, 9	139, 9
5R-1	10	29	V2	171, 72	142, 72
5R-1	10	29	Pf	172, 32	143, 32
5R-1	10	29	V3	202, 90	173, 90
5R-2	1	188	V3b	229, 85	41, 85
5R-2	1	188	V2	154, 27	326, 27
5R-2	1	188	Pf	175, 23	347, 23
5R-2	1	188	V3a	175, 64	347, 64
5R-3	2	265	V1	147, 21	242, 21
5R-3	13	206	Pf	206, 34	0, 34
5R-3	13	206	V1	206, 34	0, 34
5R-3	13	206	Pf	236, 41	30, 41
5R-4	6	199	V2	184, 29	345, 29
5R-4	7	200	V2	169, 49	329, 49
6R-1	6	218	Pf	165, 46	307, 46
6R-1	6	218	V2	170, 49	312, 49
6R-2	9	273	V1	239, 12	326, 12
6R-3	7	200	V2	45, 61	205, 61
6R-3	7	200	Pf	48, 60	208, 60
6R-3	7	200	V1	96, 41	256, 41
7R-1	17	198	V1a	139, 11	301, 11
8R-2	3	167	1	200, 47	33, 47
10R-2	7	190	MV	205, 72	15, 72
10R-2	7	190	V1a	172, 50	342, 50
10R-2	7	190	V2	180, 80	350, 80
10R-3	9	202	V3	48, 78	206, 78
10R-3	9	202	Af	184, 35	342, 35
10R-3	9	202	Pf	184, 35	342, 35
10R-3	9	202	V2	184, 35	342, 35
10R-4	7	233	V0	80, 30	207, 30
10R-4	7	233	Pf	185, 33	312, 33
10R-4	7	233	V3	208, 64	335, 64
11R-1	4	38	V0	182, 90	144, 90
11R-1	4	38	V1	183, 56	145, 56
11R-1	4	38	Pf	11, 46	333, 46
11R-1	13	199	Pf	157, 51	318, 51
11R-1	13	199	V2	160, 50	321, 50
11R-2	3	224	V2	167, 41	303, 41
11R-2	3	224	V1b	189, 80	325, 80
11R-2	4	224	Pf	172, 48	308, 48
11R-2	4	224	V2	172, 48	308, 48
11R-2	4	224	V1b	180, 93	16, 9
11R-2	4	224	V1a	183, 65	319, 65
11R-3	1	210	Pf	157, 43	307, 43
11R-3	1	210	V2	157, 43	307, 43
11R-3	1	210	Pf	161, 33	311, 33
11R-3	4	192	Pf	149, 39	317, 39
11R-3	4	192	V2	149, 39	317, 39
11R-3	4	192	Pf	166, 38	334, 38
12R-1	6	182	Pf	47, 28	225, 28
12R-2	11	205	V2	160, 37	315, 37
12R-2	11	205	Pf	178, 28	333, 28
12R-3	3	235	V2	206, 43	331, 43
12R-3	4	246	Pf	191, 39	305, 39
12R-3	4	246	V2	212, 37	326, 37
12R-4	2	219	Pf	169, 24	310, 24
12R-4	2	219	V1	178, 82	319, 82
12R-4	4	234	Pf	165, 23	291, 23
12R-4	4	234	V2	195, 25	321, 25
12R-5	3	120	V2	105, 56	345, 56
12R-5	7	246	Pf	146, 43	260, 43
12R-5	7	246	Af	180, 32	294, 32
12R-5	7	246	V2	180, 32	294, 32
13R-2	3	270	Af	180, 30	270, 30
13R-2	3	270	Pf	180, 30	270, 30
13R-2	3	270	V1	180, 30	270, 30
13R-2	3	270	V2	180, 30	270, 30
13R-3	19	176	V0	194, 84	18, 84
13R-3	19	176	Af	221, 23	45, 23
13R-3	19	176	Pf	221, 23	45, 23
13R-3	19	176	Vb	221, 23	45, 23
13R-3	19	176	V3	18, 87	202, 87
13R-4	6	188	V1a	323, 61	135, 61
13R-4	6	188	Af	170, 30	342, 30
13R-4	6	188	Pf	170, 30	342, 30
13R-4	6	188	V1b	170, 30	342, 30
14R-3	3	110	V1	21, 16	271, 16
14R-3	4	338	V2	351, 30	13, 30
14R-3	4	338	V1b	172, 43	194, 43
14R-3	4	338	V3a	0, 44	22, 44
14R-4	8	160	V1	322, 37	162, 37
14R-5	5	212	Af	175, 24	323, 24
14R-5	5	212	Pf	175, 24	323, 24
14R-5	5	212	V2	175, 24	323, 24
14R-5	7	52	V2b	152, 17	100, 17
14R-5	7	52	Af	344, 68	292, 68
14R-5	7	52	Pf	344, 68	292, 68
14R-5	7	52	V2a	344, 68	292, 68
15R-1	4	188	V1d	192, 80	4, 80
15R-1	4	188	V1c	2, 48	174, 48
15R-1	4	188	V1a	3, 49	175, 49
15R-1	4	188	V2	177, 55	349, 55
15R-1	4	188	V1b	0, 17	172, 17
15R-2	3	214	V1	12, 87	158, 87
15R-2	3	214	V2	171, 28	317, 28
15R-3	3	206.	MV	266, 35	60, 35
15R-3	3	206.	V3	30, 59	184, 59
15R-4	3	209	V2	160, 70	311, 70
15R-6	5	295	J1	170, 85	235, 85
15R-6	5	295	J2	218, 6	283, 6
15R-6	5	295	J3	245, 26	310, 26
15R-6	5	295	V2	255, 55	320, 55
16R-1	5	206	Pf	150, 30	304, 30
16R-2	1	231	Pf	144, 43	273, 43
16R-2	1	231	V2	171, 42	300, 42
16R-3	1	250	V1	359, 69	109, 69
16R-4	1B	185	V2	189, 29	4, 29
16R-4	1B	185	Pf	205, 41	20, 41
16R-4	1B	185	V1	296, 60	111, 60
16R-4	1B	185	V3	143, 56	318, 56
16R-4	1C	185	Pf	205, 41	20, 41
16R-4	1C	185	V2	212, 43	27, 43
16R-4	1C	185	V1	235, 75	50, 75
16R-5	1	253	Pf	163, 23	270, 23
16R-5	1	253	V2	167, 29	274, 29
16R-5	4	224	V2	161, 21	297, 21
16R-5	4	224	V0	0, 75	136, 75
16R-7	6	278	V2	145, 12	227, 12
16R-7	6	278	Pf	214, 11	296, 11
16R-7	6	278	MV	260, 40	342, 40
17R-1	1	347	MV	142, 22	155, 22
17R-1	1	347	V2	172, 32	185, 32
17R-3	1	222	Pf	235, 45	13, 45
17R-3	1	222	V2	235, 45	13, 45
17R-3	1	222	V0	120, 63	258, 63
17R-4	3	229	Af	225, 39	356, 39
17R-4	3	229	Pf	225, 39	356, 39
17R-4	3	229	V2	225, 39	356, 39
17R-4	3	229	V3	225, 39	356, 39
18R-2	9	295	V2a	5, 82	70, 82
18R-2	9	295	Pf	248, 37	313, 37
18R-2	9	295	V0	248, 37	313, 37
19R-1	3	213	V1	8, 88	155, 88
19R-1	3	213	Pf	147, 21	294, 21
19R-1	3	213	V2	147, 21	294, 21
19R-2	1	195	V1	242, 61	47, 61
20R-1	13	197	V1	18, 58	181, 58
20R-1	13	197	V0	156, 31	319, 31
20R-2	1A	201	V2	141, 6	300, 6
20R-2	1B	201	Pf	220, 37	19, 37
20R-3	1	246	V1a	187, 22	301, 22
20R-3	1	246	V22	30, 44	344, 44
20R-3	1	246	V1b	0, 78	114, 78
20R-3	2A	248	V2	269, 37	21, 37
20R-3	2A	248	F2	83, 57	35, 57
20R-3	2A	248		L:357/40	L:109/40
20R-3	2A	248	V3	225, 15	337, 15
20R-3	2C	248	V1a	212, 86	324, 86
20R-3	2C	248	V2	220, 27	332, 27
20R-3	2C	248	V3	240, 8	352, 8
20R-4	3A	203	V3	173, 57	330. 57
20R-4	3A	203	V1a	178, 61	335, 61
20R-4	3A	203	V2	202, 41	359, 41
20R-4	3B	203	V2	250, 37	47, 37
20R-4	3B	203	V1a	202, 47	359, 47
20R-5	4	180	Pf	4, 52	184, 52
20R-5	4	180	V1	10, 85	190, 85
20R-5	4	180	V2	29, 65	209, 65
21R-2	1	197	V1	328, 68	131, 68
21R-3	1	232	V2	345, 85	113, 85
21R-3	1	232	Af	135, 15	263, 15
21R-3	1	232	Pf	135, 15	263, 15
21R-3	1	232	V2	135, 15	263, 15
21R-3	1	232	V1b	158, 52	86, 5
21R-3	1	232	V1a	172, 80	300, 80
21R-4	6	222	V1a	184, 28	322, 28
21R-4	6	222	Af	195, 26	333, 26
21R-4	6	222	Pf	195, 26	333, 26
21R-4	6	222	V2	195, 26	333, 26
22R-2	1	249	Af	264, 9	15, 9
22R-2	1	249	V2	264, 9	15, 9
22R-2	1	249	Pf	163, 10	274, 10
22R-2	1B	249	V1b	293, 83	44, 83
22R-2	1C	249	Pf	173, 17	284, 17
22R-2	1C	249	V2	173, 17	284, 17
22R-2	1D	249	Pf	170, 16	281, 16
22R-3	1A	216	V1a	178, 65	322, 65
22R-3	1B	216	V2	299, 10	83, 10
22R-3	1B	216	CL	166, 83	10, 8
22R-3	1B	216	V3	202, 79	346, 79
22R-4	1	170	Pf	127, 46	317, 46
22R-4	1A	170	V2	166, 41	356, 41
22R-5	6	203	V2	5, 89	162, 89
22R-5	6	203	V1	10, 85	167, 85
22R-5	6	203	V3a	186, 78	343, 78
22R-6	2	223	V2	227, 87	4, 87
22R-6	2	223	MV	339, 44	116, 44
22R-6	2	223	V2	340, 12	117, 12
22R-7	8	180	V0	180, 11	0, 11
22R-7	8	180	MV	357, 79	177, 79
22R-7	8	180	V2	117, 40	297, 40

Notes: The correction factor is equal to 360° – D (the uncorrected stable remanent declination). Therefore, the corrected orientations are in the system where north is parallel to the remanent declination. Char. declin. = characteristic declination, uncorr. = uncorrected, corr. = corrected. Feature abbreviations are described in Shipboard Scientific Party (1995a) and in other portions of this volume (Dilek, Coulton, et al., this volume).

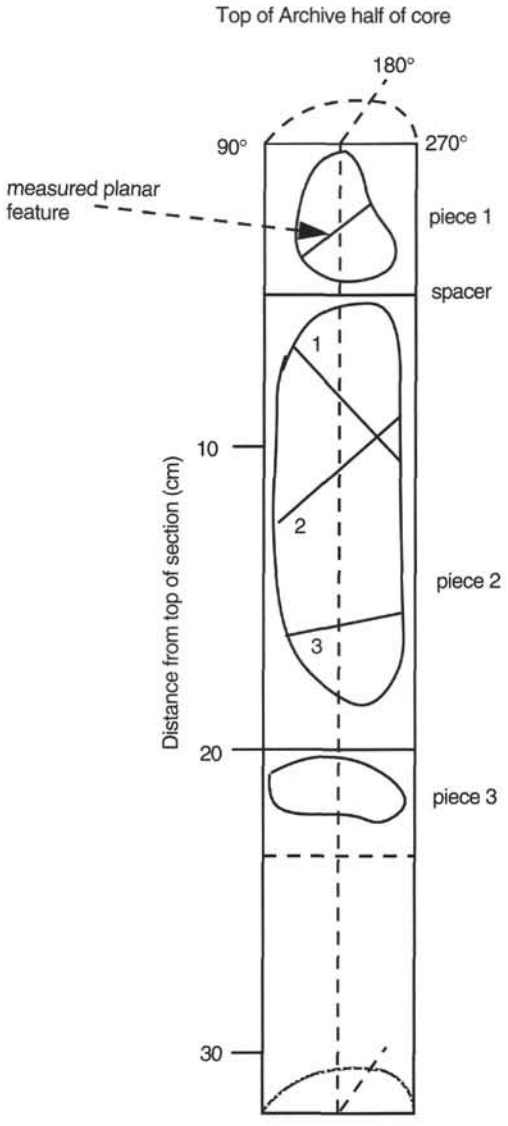

Figure 3. Sketch of the coordinate system for measuring features in ODP core. Minicores for paleomagnetic analysis were drilled from the working half of the core with the axis of the minicore cylinder aligned along the 0° direction. Measured declinations were converted to this core reference frame and then used to reorient structural features on a piece-by-piece basis.

the declination. For example, a 14° counterclockwise rotation about a 340° axis would change a 41° inclination to 35°, and at the same time change the declination from 0° to 10°. Therefore, if the inclination discrepancy is due entirely to rotations about north-south-trending axes, and the characteristic declination is assumed to be defined by a geocentric axial dipole field, then returning the characteristic declination to 0° will add a significant error to the reorientation of the core.

Despite the significant uncertainties associated with the unknown effects of anisotropy and tectonic rotation on the remanent declination, we assumed that the observed declination for each discrete sample was originally 0°. Reorientation of these samples (Site 920) involves subtracting the measured declination from any azimuth measurement done in the ODP core reference frame (Fig. 3). Stereographic projections of the reoriented major fabric in core from Site 920 show there to be a strong clustering of the poles to the crystal-plastic and V2 vein set, which comprise a planar fabric. This clustering indicates that this mesoscopic fabric has a consistent orientation downhole and between holes.

RESULTS

After reorientation, the mesoscopic crystal-plastic foliation and V2 vein set are strongly clustered with north-northwest strikes and east-northeast dips. The east-northeast dip of the foliation is parallel to in situ observations of a generally east-dipping fabric in nearby serpentinite outcrop by submersibles and towed cameras (Karson and Dick, 1983; Cannat et al., 1995; J. Miller, unpubl. data). Paleomagnetic measurements on two oriented samples collected at Site 920 during an *Alvin* dive in the spring of 1995 produced disparate results (Fig. 6A). However, one sample had a measured declination of 336° and an inclination of 42°; the direction is similar to the present-day International Geomagnetic Reference Field at the site. The submersible samples show similar fabric elements and magnetic properties as samples from Site 920 core. The discrepancy in results from the two submersible samples is more likely to be from misorientation of the sample upon recovery after the *Alvin* dive. Attempts to collect oriented samples during *Alvin* dives usually result in high failure rates because of ambiguity about which sample surfaces were measured and undulating rock surfaces that make reorientation subject to large errors.

There is no significant difference in the distribution of reoriented planar structures when data from each hole are analyzed separately. Magmatic veins (MV) and an early generation of mineralized veins (V0; Fig. 6C) generally scatter with no preferred orientation. These early veins consist usually of coarse-grained mafic minerals that are considered to be late-stage melt segregations (Cannat, Ceuleneer, et al., this volume), and that tend to cut the core at random orientations (Shipboard Scientific Party, 1995b). Two other vein generations, an early set (V1) that is cut by V2 veins and a vein set (V3) that typically cuts the V2 veins at a steep angle (Fig. 6D), are observed in the core. In general, there is no clustering of the orientations of the V1 vein set; however, the V3 set has a subtle clustering that results in dips to the northeast with very few, if any, strike orientations in that quadrant. Some of the scatter in plots incorporating data from different vein sets may reflect the misinterpretation and misassignment of the measured vein to a specific set. Not all the vein sets were present along all intervals of core. Particularly, if the V2 vein set was not well developed, then the most common crosscutting relationships could not be well established and classification was purely on the basis of the appearance of the vein on the cut surface of the core.

In Hole 920B, the plastic fabric is nearly always parallel to the orientation of the V2 vein set. The strike of V2 veins are consistently north-northwest, although in the middle of shipboard Unit 3 (35–85 mbsf), there is a cluster that strikes north-northeast (Fig. 7). Coincident with this cluster is an increase in the dip of the V2 veins. In general, the V3 veins show steeper dips, except near the same location downhole in Unit 3, where some relatively shallow dips were observed.

V2 veins in core from Hole 920D (Fig. 8) show more variation in both strike and dip than those in core from Hole 920B. In the upper part of Hole 920D, the vein orientations are similar to that in Hole 920B, and the crystal-plastic fabric is generally parallel to the V2 veins. Below 110 m depth, the strike and dip of both V2 and the plastic fabric vary more strongly and substantially diverge from each other. The development of V2 veins is sparse in many intervals of core below this depth. The interpretation of these patterns and the significance of the vein generations at Site 920 is discussed in Dilek, Coulton, et al. (this volume). Measurements of faults, joints, lineations, and structural elements other than plastic fabric and veins are too sparse for any general interpretations to be made; however, their orientations are included in Tables 1 and 2.

Structural features in the gabbro cores are much less common and more difficult to measure accurately, partly because much of the magmatic and plastic deformation pervasive in these cores is weakly developed (Shipboard Scientific Party, 1995c, 1995d). The magnetic behavior of the samples taken from gabbroic rocks is also much more complicated (Gee et al., this volume). Some gabbro samples from

Table 3. Anisotrophy of magnetic susceptibility (AMS) data for Holes 920B and 920D.

Core, section, interval (cm)	Depth (mbsf)	AMS			Char. declin. (uncorr.)	AMS directions, reoriented					
		K_1/K_3	K_1/K_2	K_2/K_3		K_1 declin.	K_1 inclin.	K_2 declin.	K_2 inclin.	K_3 declin.	K_3 inclin.
153-920B-											
1W-1, 55–58	0.55	1.2030	1.0780	1.1160	244.0	123.4	51.6	7.7°	18.9	265.3	31.9
1W-2, 24–27	1.29	1.1140	1.0170	1.0950	181.0	21.5	28.7	125.8	24.2	249.3	50.8
1W-3, 46–49	2.94	1.1110	1.0450	1.0640	187.5	21.1	17.5	119.2	23.9	258.3	59.7
1W-3, 73–76	3.21	1.1583	1.0499	1.1032	34.0	46.9	27.3			286.1	44.7
1W-3, 76–79	3.24	1.1716	1.0641	1.1010	54.0	50.0	26.1			262.8	59.8
2R-1, 17–20	14.17	1.1090	1.0350	1.0710	294.2	359.1	3.0	89.7	11.7	255.1	77.8
3R-1, 65–68	24.15	1.2190	1.0560	1.1540	193.1	5.4	9.3	107.5	52.2	268.6	36.2
3R-2, 36–39	25.36	1.1200	1.0730	1.0440	163.6	0.9	7.8	99.2	46.2	263.7	42.7
3R-2, 79–83	25.79	1.1510	1.1048	1.0415	194.0	211.5	12.9			117.6	16.2
3R-2, 91–94	25.91	1.2114	1.0946	1.1670	194.0	212.2	24.9	315.5	58.5	113.6	18.0
3R-2, 98–101	25.98	1.2130	1.0850	1.1170	196.5	15.1	19.0	141.7	60.0	277.1	22.3
4R-1, 60–63	33.80	1.1070	1.0500	1.0540	266.5	16.8	27.3	146.6	51.2	272.6	25.3
5R-1, 52–55	43.22	1.1700	1.1110	1.0530	217.5	3.91	5.81	50.97	1.42	71.1	9.6
5R-2, 60–63	44.74	1.1880	1.0460	1.1350	204.8	21.0	27.0	130.5	33.2	260.8	44.6
5R-3, 61–64	46.23	1.0880	1.0580	1.0290	207.2	6.6	13.3	250.4	61.8	102.8	24.4
5R-3, 99–102	46.61	1.1890	1.0940	1.0870	182.7	4.2	6.4	105.6	60.5	270.7	28.7
6R-3, 21–23	55.05	1.0890	1.0490	1.0380	228.2	11.2	43.4	188.4	46.6	279.9	1.4
6R-3, 23–26	55.08	1.0730	1.0240	1.0470	239.1	22.0	40.2	127.1	17.2	235.1	44.8
6R-3, 57–60	55.42	1.0640	1.0540	1.0100	222.1	187.6	24.6	46.5	59.5	285.6	16.8
7R-1, 20–23	61.20	1.1307	1.0451	1.0819	232.0	258.8	26.9	36.9	55.8	158.4	19.6
7R-1, 23–26	61.23	1.0957	1.0395	1.0541	217.0	253.3	20.1	7.2	47.9	148.3	35.2
7R-1, 55–58	61.55	1.1980	1.1200	1.0700	209.5	15.11	1.31	40.8	71.1	282.0	14.9
7R-2, 5–8	62.47	1.2660	1.0280	1.2310	176.2	358.9	0.28	9.15	3.52	68.83	6.5
7R-2, 42–45	62.84	1.2390	1.0970	1.1300	194.7	169.2	0.97	8.24	8.52	60.04	1.5
7R-2, 91–94	63.33	1.1860	1.0480	1.1320	178.3	174.9	0.7	84.0	53.4	265.5	36.5
7R-3, 15–18	63.98	1.1580	1.0520	1.1000	193.1	157.2	10.5	55.9	46.5	256.6	41.5
8R-1, 81–84	71.21	1.1734	1.0474	1.1202	181.0	182.0	2.4	279.0	71.1	91.2	18.7
8R-1, 84–87	71.24	1.2089	1.0605	1.1400	183.0	356.9	14.2	235.4	64.1	92.5	21.2
8R-2, 24–27	71.92	1.2540	1.0490	1.1960	195.0	167.9	3.1	75.1	42.5	261.2	47.4
8R-2, 70–73	72.38	1.1260	1.0650	1.0570	187.0	197.7	4.3	292.9	49.7	104.1	39.9
8R-2, 73–76	72.41	1.0740	1.0410	1.0320	187.0	189.9	12.3	63.5	69.8	283.4	15.7
8R-3, 69–72	73.71	1.1700	1.0560	1.1080	190.2	1.7	0.2	91.9	53.4	271.6	36.7
8R-3, 115–118	74.17	1.1560	1.1000	1.0500	214.8	10.2	29.4	133.3	44.1	260.0	31.6
8R-3, 118–121	74.20	1.1520	1.0600	1.0870	213.8	10.6	32.7	155.2	51.8	268.9	17.6
8R-4, 11–14	74.48	1.1230	1.0180	1.1040	189.0	25.9	26.9	178.0	60.2	289.7	11.9
8R-4, 17–20	74.54	1.1408	1.0020	1.1385	180.0	201.8	24.3	328.2	52.7	98.92	6.4
8R-4, 29–32	74.66	1.1351	1.0129	1.1206	191.0	219.0	66.2	14.9	21.9	108.5	8.8
8R-5, 62–65	76.36	1.1920	1.0590	1.1250	185.2	9.2	10.8	113.8	53.1	271.5	34.8
9R-1, 41–44	80.11	1.1380	1.1070	1.0280	200.4	8.3	14.4	149.3	71.7	275.4	11.0
9R-2, 36–39	81.52	1.1110	1.0460	1.0620	236.7	14.8	24.4	130.9	44.1	265.6	36.0
9R-2, 39–42	81.55	1.1040	1.0500	1.0510	236.7	17.2	38.9	133.1	28.5	248.2	38.0
9R-2, 69–72	81.85	1.1144	1.0439	1.0676	202.0	25.1	54.2	190.9	35.0	285.6	6.8
9R-2, 72–75	81.88	1.1106	1.0360	1.0721	212.0	212.4	59.4	13.9	29.3	108.5	8.1
9R-2, 84–87	82.00	1.1480	1.0070	1.1400	194.7	353.1	65.6	172.3	24.3	262.4	0.3
9R-2, 87–90	82.03	1.1390	1.0220	1.1140	194.9	349.3	50.9	153.2	38.0	249.4	8.0
10R-1, 17–20	89.27	1.2010	1.0480	1.1460	216.8	339.8	1.3	71.6	55.9	249.0	34.1
10R-1, 20–23	89.30	1.2120	1.0050	1.2060	216.8	156.8	15.4	37.3	60.7	254.0	24.3
10R-2, 2–5	90.48	1.0690	1.0320	1.0360	192.5	180.5	3.0	83.5	66.5	271.7	23.3
10R-2, 37–40	90.83	1.1154	1.0295	1.0835	220.0	249.3	46.6	0.5	18.9	105.5	37.3
10R-2, 63–66	91.09	1.3030	1.0247	1.2716	200.0	228.8	52.9	351.9	22.4	94.5	27.8
10R-2, 70–73	91.16	1.2960	1.0630	1.2200	207.7	353.4	16.3	111.8	58.5	255.1	26.1

Sites 921 to 924 do have a relatively simple demagnetization behavior, where a single characteristic component of magnetization can be identified with an inclination near the expected value of 41°. Veins from Hole 923A have been reoriented using the same method as for Site 920 and using only data where this characteristic inclination is near 41° (Fig. 9). Although the number of structures including both magmatic fabrics and metamorphic foliations as well as veins is low, the bulk of them have a gentle dip to the northeast after reorientation (Table 4). Again, this is consistent with structural evidence from dive programs, and is an indication that, with further work on gabbro samples to isolate characteristic magnetization components, it should be possible to reorient many more features in core from Holes 921A to 924C.

CONCLUSIONS

The reorientation of planar features in Site 920 cores using a characteristic remanent declination of the magnetization shows that major pervasive structural fabric elements in the core have a consistent orientation that dips to the east-northeast. Submersible studies have shown that surface outcrops of the serpentinites commonly have a gently east-dipping structure defined by a disjunctive, anastomosing foliation similar to that observed in the core from Site 920. This consistency indicates that the reorientation procedure is reasonably valid for these rocks.

The V2 veins and crystal-plastic fabric reflect deformation in at least two different temperature and pressure regimes. However, only serpentinization and possible later magnetization events, including the creation of the V2 serpentine vein set, affected the acquired remanence. A high anisotropy of susceptibility is observed in these samples, probably caused by preferred orientation of magnetite grains or grain clusters formed during the serpentinization (Lawrence et al., this volume). This anisotropy may account for part of the discrepancy between measured inclinations (35.2 ± 1) and the expected geocentric axial dipole inclination (41°) for the site.

Although the major fabric elements generally show consistent orientations throughout the core, other less conspicuous structural features show no obvious relationship to the major foliations or each other. Vein sets other than the V2 set generally have randomly scattered orientations overall, with no discernible relationship to depth in the recovered core or rock type.

There is generally a more diverse set of structural elements in the gabbros recovered from Sites 921 to 924. Preliminary reorientation of some of these elements in core from Hole 923A indicates an east-northeast dip of many of these structures, which is consistent with the regional trends and local submersible observations of gabbro exposures.

Table 3 (continued).

Core, section, interval (cm)	Depth (mbsf)	AMS			Char. declin. (uncorr.)	AMS directions, reoriented					
		K_1/K_3	K_1/K_2	K_2/K_3		K_1 declin.	K_1 inclin.	K_2 declin.	K_2 inclin.	K_3 declin.	K_3 inclin.
10R-3, 120–123	93.07	1.1640	1.0240	1.1370	189.1	177.8	0.5	80.9	86.6	267.8	3.4
10R-4, 64–67	93.95	1.1820	1.0320	1.1450	222.9	175.0	16.4	49.9	62.8	271.5	21.0
10R-5, 13–16	94.87	1.1130	1.0440	1.0660	208.3	170.7	38.5	39.8	39.5	284.7	27.1
11R-1, 15–18	98.65	1.1343	1.0284	1.1030	222.0	264.0	36.1	173.8	0.2	83.5	53.9
11R-1, 57–60	99.07	1.3010	1.0429	1.2475	212.0	247.0	36.5	359.4	27.3	116.4	41.4
11R-1, 70–73	99.20	1.2690	1.0500	1.2080	206.2	7.8	17.4	113.3	40.4	259.9	44.6
11R-1, 119–122	99.69	1.2320	1.0260	1.2010	250.8	5.1	12.0	119.9	63.0	269.7	23.8
11R-1, 122–125	99.72	1.2260	1.0290	1.1910	250.8	9.6	24.4	132.6	50.2	264.9	29.3
11R-2, 10–13	100.06	1.2860	1.0530	1.2210	206.0	1.6	10.2	102.4	46.1	262.3	42.1
12R-1, 51–54	108.21	1.1680	1.0210	1.1430	245.8	62.7	46.7	168.4	14.3	270.7	39.8
12R-1, 66–69	108.36	1.1746	1.0785	1.0891	246.0	253.0	22.1	16.3	53.5	150.8	27.4
12R-1, 76–79	108.46	1.1566	1.0553	1.0959	246.0	270.9	15.1	20.9	51.7	170.4	34.2
12R-1, 100–103	108.70	1.1810	1.0510	1.1240	183.1	106.0	40.7	325.3	42.0	215.2	20.9
12R-2, 50–53	109.65	1.1800	1.0250	1.1510	193.6	132.7	47.3	7.1	28.2	259.8	29.1
12R-2, 113–116	110.28	1.2376	1.0437	1.1858	193.0	5.9	13.8	260.6	47.0	107.6	39.7
12R-2, 117–120	110.32	1.1961	1.0351	1.1555	192.0	11.5	0.4	280.3	70.7	101.6	19.3
12R-2, 126–129	110.41	1.2276	1.0476	1.1718	244.0	50.7	23.6	278.5	57.0	150.7	21.7
12R-2, 129–132	110.44	1.1513	1.0418	1.1051	251.0	49.1	32.2	267.4	51.2	151.7	19.2
12R-3, 26–29	110.91	1.2468	1.0144	1.2292	202.0	2.1	36.1	228.4	43.5	112.1	25.1
12R-3, 29–32	110.94	1.3040	1.0370	1.2574	193.0	197.0	9.5	325.3	74.9	105.0	11.6
12R-3, 80–83	111.45	1.2640	1.0370	1.2180	224.0	9.3	21.4	122.8	45.4	262.2	36.9
12R-4, 80–83	112.52	1.2160	1.0250	1.1860	197.0	332.4	1.2	63.4	37.8	240.9	52.2
12R-5, 10–13	113.10	1.2410	1.0470	1.1850	214.3	30.6	16.7	146.9	56.0	291.1	28.7
12R-5, 13–16	113.13	1.1940	1.0780	1.1070	214.3	87.9	43.1	309.7	38.5	200.6	22.4
12R-6, 16–19	114.52	1.2010	1.0350	1.1610	196.9	40.3	48.8	140.6	9.0	238.1	39.7
13R-1, 60–63	117.80	1.2050	1.0450	1.1530	204.8	13.3	17.8	113.5	28.7	255.8	55.2
13R-1, 94–97	118.14	1.2670	1.0810	1.1720	211.0	32.3	27.4	130.5	15.4	246.5	57.9
13R-2, 80–83	119.37	1.2360	1.0520	1.1740	223.9	358.5	3.0	91.4	44.5	265.5	45.4
13R-2, 95–98	119.52	1.1457	1.0335	1.1085	213.0	260.2	33.3	5.2	21.5	121.9	48.7
13R-2, 99–102	119.56	1.2257	1.0238	1.1973	228.0	41.8	1.6	310.3	42.4	133.5	47.6
13R-3, 36–39	120.25	1.1020	1.0060	1.0960	230.4	71.5	21.2	333.2	20.4	203.3	59.9
13R-4, 23–26	121.51	1.0330	1.0160	1.0170	5.7	154.7	22.5	32.1	52.3	257.7	28.4
153-920D-											
2R-1, 21–24	8.21	1.1270	1.0360	1.0890	134.3	–4.2	20.6	123.1	58.2	–103.4	23.1
2R-1, 24–27	8.24	1.1130	1.0530	1.0570	118.2	192.7	12.0	89.0	48.1	-67.3	39.4
2R-1, 116–119	9.16	1.0820	1.0490	1.0320	164.2	–84.1	73.5	14.4	2.5	105.1	16.3
3R-2, 49–52	19.49	1.1470	1.0310	1.1120	170.6	45.3	17.7	–46.6	7.0	–157.6	71.0
4R-1, 22–25	27.52	1.1630	1.0990	1.0590	222.8	9.3	16.0	–81.2	1.7	–176.9	73.9
4R-2, 17–20	28.77	1.1040	1.0500	1.0520	214.2	71.8	72.0	–30.2	4.0	–21.2	17.0
4R-2, 43–46	29.03	1.1040	1.0434	1.0582	318.0	–139.2	35.8	–29.7	24.8	86.8	43.9
4R-3, 35–38	30.19	1.1900	1.0080	1.1800	207.4	23.5	28.6	157.9	52.0	–79.7	22.7
5R-1, 56–59	37.46	1.1560	1.1010	1.0500							
5R-2, 33–36	38.24	1.0810	1.0120	1.0690	188.2						
5R-2, 36–39	38.27	1.1410	1.0190	1.1190	188.2	42.4	17.8	–51.8	12.7	–175.5	67.9
5R-3, 20–23	39.47	1.0940	1.0890	1.0050	265.3	–6.2	20.3	94.9	27.6	–127.7	54.6
5R-3, 127–130	40.54	1.2700	1.0270	1.2360	205.9	6.5	13.5	101.2	18.8	-117.1	66.5
5R-4, 93–96	41.66	1.1180	1.0660	1.0490	145.7	26.3	19.8	–74.2	26.7	148.3	55.7
6R-1, 53–56	47.03	1.1850	1.1390	1.0400	217.7	7.4	2.4	98.5	26.5	–87.5	63.4

REFERENCES

Bonatti, E., 1976. Serpentinite protrusions in the oceanic crust. *Earth Planet. Sci. Lett.,* 32:107–113.

Cannat, M., 1993. Emplacement of mantle rocks in the seafloor at mid-ocean ridges. *J. Geophys. Res.,* 98:4163–4172.

Cannat, M., Karson, J.A., Miller, D.J., et al., 1995. *Proc. ODP, Init. Repts.,* 153: College Station, TX (Ocean Drilling Program).

Cannat, M., Mével, C., Maia, M., Deplus, C., Durand, C., Gente, P., Agrinier, P., Belarouchi, A., Dubuisson, G., et al., 1995. Thin crust, ultramafic exposures, and rugged faulting patterns at the Mid-Atlantic Ridge (22°–24°N). *Geology,* 23:49–52.

Cannat, M., and Pariso, J., 1991. Partial reorientation of the deformational structures at Site 735 using paleodeclination measurements. *In* Von Herzen, R.P., Robinson, P.T., et al., *Proc. ODP, Sci. Results,* 118: College Station, TX (Ocean Drilling Program), 409–414.

Karson, J.A., 1990. Seafloor spreading on the Mid-Atlantic Ridge: implications for the structure of ophiolites and oceanic lithosphere produced in slow-spreading environments. *In* Malpas, J., Moores, E.M., Panayiotou, A., and Xenophontos, C. (Eds.), *Ophiolites: Oceanic Crustal Analogues:* Proc. Symp. "Troodos 1987": Nicosia, Cyprus (Minist. Agric. Nat. Resour.), 547–555.

Karson, J.A., and Dick, H.J.B., 1983. Tectonics of ridge-transform intersections at the Kane Fracture Zone. *Mar. Geophys. Res.,* 6:51–98.

Kirschvink, J.L., 1980. The least-squares line and plane and the analysis of palaeomagnetic data. *Geophys. J.R. Astron. Soc.,* 62:699–718.

McFadden, P.L., and Reid, A.B., 1982. Analysis of palaeomagnetic inclination data. *Geophys. J.R. Astron. Soc.,* 69:307–319.

Schultz, N.J., Detrick, R.S., and Miller, S.P., 1988. Two- and three-dimensional inversion of magnetic anomalies in the MARK area (Mid-Atlantic Ridge, 23 N). *Mar. Geophys. Res.,* 10:41–57.

Shipboard Scientific Party, 1995a. Explanatory notes. *In* Cannat, M., Karson, J.A., Miller, D.J., et al., *Proc. ODP, Init. Repts.,* 153: College Station, TX (Ocean Drilling Program), 15–42.

———, 1995b. Site 920. *In* Cannat, M., Karson, J.A., Miller, D.J., et al., *Proc. ODP, Init. Repts.,* 153: College Station, TX (Ocean Drilling Program), 45–119.

———, 1995c. Site 921. *In* Cannat, M., Karson, J.A., Miller, D.J., et al., *Proc. ODP, Init. Repts.,* 153: College Station, TX (Ocean Drilling Program), 121–177.

———, 1995d. Site 923. *In* Cannat, M., Karson, J.A., Miller, D.J., et al., *Proc. ODP, Init. Repts.,* 153: College Station, TX (Ocean Drilling Program), 217–258.

Stacey, F.D., and Banerjee, S.K., 1974. *The Physical Principles of Rock Magnetism.* Dev. Solid Earth Geophys., 5: New York (Elsevier).

Date of initial receipt: 1 August 1995
Date of acceptance: 2 May 1996
Ms 153SR-040

Table 3 (continued).

Core, section, interval (cm)	Depth (mbsf)	AMS			Char. declin. (uncorr.)	AMS directions, reoriented					
		K_1/K_3	K_1/K_2	K_2/K_3		K_1 declin.	K_1 inclin.	K_2 declin.	K_2 inclin.	K_3 declin.	K_3 inclin.
153-920D-											
6R-2, 48–51	48.30	1.1480	1.0100	1.1360	273.3	–32.7	20.1	100.3	61.8	–129.9	19.0
6R-3, 54–57	49.60	1.1410	1.0700	1.0660	200.2	3.5	40.7	–118.3	31.5	127.9	33.3
8R-1, 141–144	67.31	1.2720	1.0220	1.2450	4.0	159.4	14.2	12.2	73.3	251.7	8.7
8R-2, 43–46	67.77	1.1360	1.0360	1.0970	167.2	–8.0	6.0	116.6	79.5	–98.9	8.5
10R-2, 87–90	80.36	1.1333	1.0841	1.0454	186.0	–150.0	82.1	30.6	7.9	–59.4	0.1
10R-2, 90–93	80.39	1.1710	1.0590	1.1058	194.0	–162.8	71.2	13.7	18.8	104.0	1.1
10R-2, 134–137	80.83	1.1010	1.0250	1.0740	202.1	–5.1	2.9	89.0	55.0	–97.1	34.8
10R-3, 74–77	81.70	1.1950	1.0300	1.1600	201.5	6.92	9.61	60.9	57.7	–89.9	11.8
10R-3, 77–80	81.73	1.2020	1.0190	1.1800	201.5						
10R-4, 80–83	83.24	1.2220	1.0800	1.1320	233.2	4.1	38.4	112.9	22.1	–134.6	43.4
11R-1, 27–30	85.57	1.2180	1.0350	1.1770	37.6	0.3	5.8	93.5	29.2	260.2	60.1
11R-1, 125–128	86.55	1.2640	1.0520	1.2020	198.6	173.6	7.46	7.46	5.0	–93.2	23.7
11R-2, 43–46	87.15	1.1685	1.0747	1.0873	223.0	–178.5	38.4	0.1	51.6	90.9	0.7
11R-2, 46–49	87.18	1.2450	1.0745	1.1587	225.0	179.04	1.5	–16.2	47.5	82.2	7.6
11R-2, 63–66	87.35	1.2010	1.0330	1.1620	223.7	21.8	30.6	127.1	24.0	–111.7	49.3
11R-2, 66–69	87.38	1.2160	1.0190	1.1930	223.7						
11R-3, 6–9	87.98	1.2395	1.0111	1.2259	215.0	–162.6	33.1	–25.8	48.2	91.7	22.4
11R-3, 9–12	88.01	1.1960	1.0103	1.1838	206.0	41.7	45.0	178.6	36.1	–73.4	23.0
11R-3, 22–25	88.14	1.2340	1.0500	1.1750	222.3						
11R-3, 25–28	88.17	1.1730	1.0260	1.1430	222.3	72.0	53.9	164.8	2.0	–103.8	36.0
11R-3, 49–52	88.41	1.1123	1.0050	1.1067	192.0	–109.4	71.0	10.0	9.6	102.8	16.3
11R-3, 52–55	88.44	1.2071	1.0139	1.1905	192.0	–153.4	14.2	25.3	75.8	116.6	0.3
12R-1, 104–107	96.04	1.2590	1.0770	1.1690	181.7	159.9	3.9	67.7	29.1	–103.3	60.6
12R-2, 119–122	97.64	1.2620	1.0380	1.2160	205.2	151.9	25.0	38.1	40.9	–96.1	38.8
12R-3, 65–68	98.38	1.2899	1.0494	1.2292	241.0	–163.2	30.6	–36.6	45.3	87.6	29.1
12R-3, 68–70	98.41	1.2932	1.0373	1.2466	229.0	–156.1	48.3	–4.5	38.1	97.1	14.4
12R-3, 86–89	98.59	1.2400	1.0730	1.1550	246.2	–2.9	14.8	98.6	37.2	–110.6	49.0
12R-4, 54–57	99.57	1.1190	1.0350	1.0820	219.1	–22.2	3.9	71.3	41.1	–116.6	48.6
12R-4, 103–106	100.06	1.2818	1.1052	1.1598	234.0	–107.3	33.4	161.3	2.2	68.0	56.5
12R-4, 107–110	100.10	1.2504	1.0995	1.1372	236.0	–112.4	32.1	155.8	2.9	61.2	57.7
12R-5, 26–29	100.79	1.3200	1.0660	1.2370	120.2	162.7	20.9	48.9	46.7	–91.2	35.9
13R-2, 84–87	106.33	1.2130	1.1590	1.0470	270.1	–2.6	9.1	104.4	61.4	–97.2	26.9
13R-3, 126–129	108.19	1.2660	1.0100	1.2540	175.6	28.7	21.0	121.5	7.3	–130.4	67.7
13R-4, 41–44	108.74	1.1430	1.0730	1.0650	188.5	–170.4	10.6	92.0	35.0	–66.1	53.0
14R-1, 58–61	114.88	1.2170	1.1220	1.0860	196.3	7.9	9.2	–86.8	26.9	115.1	61.4
14R-2, 35–38	116.14	1.2359	1.0553	1.1711	220.0						
14R-2, 38–41	116.17	1.2766	1.0398	1.2277	220.0	–177.3	45.4	2.9	44.6	–87.2	0.1
14R-3, 82–85	117.85	1.1430	1.0450	1.0940	109.5	14.7	23.1	108.9	9.8	220.2	64.7
14R-3, 91–94	117.94	1.1439	1.0727	1.0664	338.0						
14R-3, 94–97	117.97	1.1737	1.0530	1.1147	338.0	–78.0	63.4	149.4	18.7	53.0	18.2
14R-4, 137–140	119.86	1.2800	1.1970	1.0690	159.8	–16.5	14.1	157.3	75.9	–106.9	1.5
14R-5, 69–72	120.59	1.3180	1.0040	1.3120	212.0	163.3	15.4	10.2	72.8	–104.7	7.4
14R-5, 106–109	120.96	1.1599	1.0149	1.1429	50.0	71.4	57.4	281.6	28.9	183.8	13.7
14R-5, 109–112	120.99	1.2623	1.0289	1.2268	55.0	72.5	44.3	294.9	37.1	186.5	22.6
15R-1, 80–83	124.70	1.3030	1.0310	1.2640	195.0	156.7	13.3	51.1	48.8	–102.6	38.1
15R-2, 92–95	126.04	1.2030	1.0330	1.1640	213.7	–1.4	10.8	101.1	48.5	–100.4	39.5
15R-3, 48–51	126.99	1.2120	1.0660	1.1380	237.6	14.7	27.4	144.6	51.0	–89.5	25.4
15R-3, 93–96	127.44	1.2732	1.0307	1.2353	206.0	–156.3	55.6	1.0	32.3	97.8	10.6

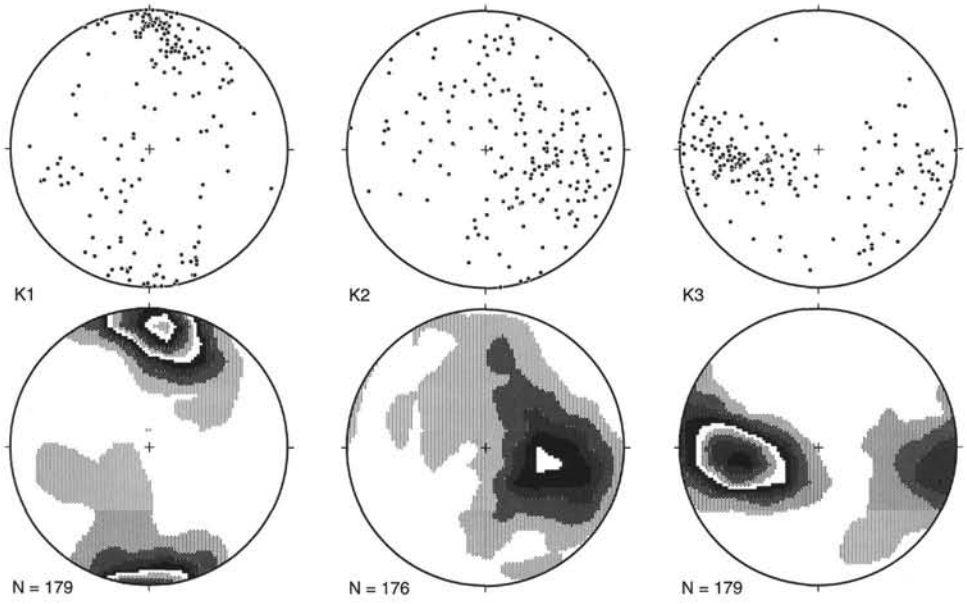

Figure 4. Lower hemisphere stereographic projection plots of the principal axes of the susceptibility ellipsoid after reorientation. The minimum susceptibility axis (K_3) dips about 30° to the west-southwest, and therefore the magnetic foliation dips to the east-northeast, approximately parallel to the orientation of the V2 vein set and the crystal-plastic fabric.

Table 3 (continued).

Core, section, interval (cm)	Depth (mbsf)	AMS K_1/K_3	AMS K_1/K_2	AMS K_2/K_3	Char. declin. (uncorr.)	AMS directions, reoriented K_1 declin.	K_1 inclin.	K_2 declin.	K_2 inclin.	K_3 declin.	K_3 inclin.
15R-3, 96–99	127.47	1.1984	1.0266	1.1674	206.0						
15R-4, 72–75	128.47	1.3160	1.0430	1.2620	208.7	–2.0	12.8	104.1	50.9	–101.6	36.2
15R-6, 76–79	131.11	1.1579	1.0505	1.1022	295.0						
15R-6, 79–82	131.14	1.1968	1.0699	1.1186	295.0	–65.1	41.6	–172.0	18.1	80.3	42.8
16R-1, 98–101	134.38	1.1730	1.0880	1.0780	206.2						
16R-1, 101–104	134.41	1.1380	1.1080	1.0270	206.2	12.7	26.5	106.3	7.2	–149.8	62.4
16R-3, 5–8	135.97	1.0810	1.0400	1.0390	249.6	9.7	4.3	105.2	52.5	–83.6	37.2
16R-4, 20–23	137.18	1.0911	1.0140	1.0761	186.0	–104.1	43.0	33.2	38.2	142.6	22.9
16R-4, 25–28	137.23	1.1225	1.0076	1.1141	184.0	8.5	66.3	–109.9	11.8	155.7	20.3
16R-4, 82–85	137.80	1.3380	1.0310	1.2970	189.2	22.0	6.8	113.7	14.0	–93.2	74.4
16R-5, 80–83	138.93	1.2350	1.0500	1.1760	223.8	–18.7	4.8	74.2	32.1	–116.2	57.5
16R-7, 54–57	141.53	1.2370	1.0640	1.1630	278.0						
16R-7, 57–60	141.56	1.2370	1.0730	1.1530	278.0	160.7	4.2	68.0	32.2	–102.7	57.5
17R-3, 37–40	145.74	1.1610	1.0430	1.1130	222.0						
17R-3, 40–43	145.77	1.1630	1.0430	1.1150	222.0	107.8	8.2	4.9	57.3	–157.2	31.4
17R-4, 103–106	147.69	1.3110	1.0480	1.2520	228.8	6.3	21.6	109.7	30.2	–113.5	51.4
18R-1, 123–126	153.83	1.1040	1.0150	1.0880	344.0	146.8	33.5	–12.4	54.7	–116.6	9.8
18R-2, 70–73	154.80	1.1526	1.0375	1.1109	296.0	–54.4	33.3	–175.7	38.3	62.0	34.1
18R-2, 83–87	154.93	1.1683	1.0419	1.1214	293.0	–48.4	32.6	–173.4	41.9	64.1	30.9
18R-3, 75–78	156.10	1.1590	1.0400	1.1140	198.2						
18R-3, 78–81	156.13	1.1260	1.0660	1.0570	198.2	2.6	9.9	107.9	56.5	–93.6	31.6
18R-4, 12–15	156.85	1.2040	1.1100	1.0840	190.8	13.4	8.6	107.2	23.9	–95.0	64.4
19R-1, 18–21	162.48	1.1580	1.1170	1.1580	212.8	–4.5	20.4	92.1	17.3	–140.8	62.7
19R-2, 13–16	163.80	1.1980	1.0760	1.1130	195.2						
19R-2, 16–19	163.83	1.1880	1.0660	1.1150	195.2	–0.2	11.1	101.8	46.6	–100.1	41.3
20R-1, 103–106	172.93	1.2130	1.1260	1.0780	197.2	17.7	23.6	117.2	20.7	–116.1	57.8
20R-1, 106–109	172.96	1.2040	1.1280	1.0680	197.2						
20R-2, 24–27	173.30	1.1960	1.1240	1.0640	200.9	10.0	24.3	110.0	21.1	–123.7	56.9
20R-3, 80–83	174.93	1.2320	1.0340	1.1910	247.8	–4.1	17.8	118.3	59.0	–102.5	24.4
20R-4, 38–41	175.92	1.1800	1.0430	1.1310	202.7	–0.5	12.5	102.5	45.5	–102.0	41.8
20R-4, 41–44	175.95	1.1320	1.0980	1.0320	202.7						
20R-5, 75–78	177.75	1.2387	1.0893	1.1371	174.0	–54.7	78.9	65.1	5.6	156.0	9.5
20R-5, 78–82	177.78	1.2417	1.0711	1.1592	185.0	–46.7	77.7	49.3	1.3	139.6	12.2
20R-5, 98–101	177.98	1.2480	1.0800	1.1560	188.8	177.5	9.0	82.4	29.2	–77.1	59.2
21R-1, 93–96	182.43	1.3740	1.0610	1.2950	205.9	0.2	3.9	94.5	47.4	–93.4	42.3
21R-2, 40–43	183.15	1.2950	1.0580	1.2240	196.7	–2.6	5.5	90.6	30.1	–102.0	59.3
21R-2, 43–46	183.18	1.2530	1.0510	1.1920	196.7						
21R-2, 97–100	183.72	1.2720	1.2310	1.0330	170.6	–7.3	4.1	85.1	31.0	–104.0	58.7
21R-3, 22–25	184.32	1.3110	1.0350	1.2660	232.2	159.9	3.6	68.5	21.5	–101.1	68.2
21R-4, 68–71	186.28	1.2040	1.0320	1.1670	222.2	15.5	11.2	113.3	34.2	–90.1	53.5
22R-2, 27–30	192.07	1.1217	1.0697	1.0487	249.0	–171.5	13.7	–53.2	62.8	92.6	23.1
22R-2, 30–33	192.10	1.1032	1.0665	1.0344	250.0	–171.7	4.3	–79.5	26.9	89.9	62.7
22R-2, 86–89	192.66	1.1900	1.0480	1.1350	260.9						
22R-2, 89–92	192.69	1.2110	1.0530	1.1510	260.9	4.5	38.9	178.7	50.9	–87.8	2.9
22R-3, 17–20	192.90	1.0580	1.0300	1.0280	215.6	6.8	9.7	126.4	70.9	–86.0	16.3
22R-4, 50–53	193.93	1.2350	1.0740	1.1500	170.4	176.3	9.4	83.1	18.2	–67.5	69.4
22R-5, 104–107	195.67	1.3420	1.0740	1.2500	201.1	3.2	7.1	94.9	13.6	–113.8	74.5
22R-5, 107–110	195.70	1.3160	1.0820	1.2170	204.6	2.0	12.1	94.8	12.8	–129.9	72.2
22R-6, 24–26	196.28	1.3485	1.0656	1.2655	218.0	–139.5	51.5	41.1	38.5	–49.1	0.3
22R-6, 26–29	196.30	1.3086	1.0617	1.2326	228.0	–155.1	65.6	29.2	24.3	–61.5	1.6
22R-6, 15–18	196.35	1.2840	1.0510	1.2220	234.0						

Notes: The correction factor is equal to 360° – D (the uncorrected stable remanent declination). Therefore, the corrected orientations are in the system where north is parallel to the remanent declination. Char. declin. = characteristic declination, inclin. = inclination, uncorr. = uncorrected, corr. = corrected.

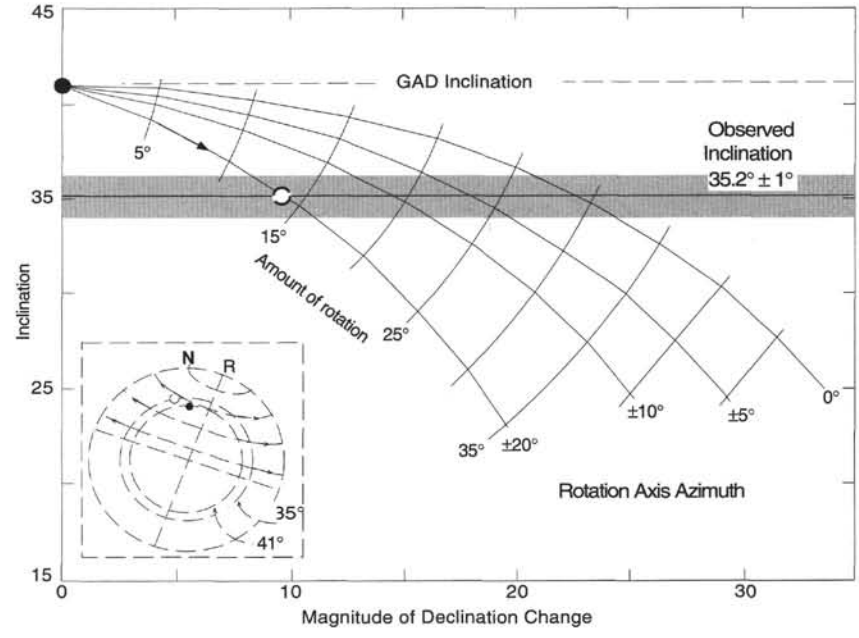

Figure 5. Diagram showing the change in both inclination and declination for a unit vector with orientation of 0° inclination and 41° declination when rotated about horizontal axes with azimuths ±20° about north. The solid circle shows the original orientation of the vector and the open circle denotes its orientation after a 14° clockwise rotation about a horizontal axis with a 20° trend or a similar counterclockwise rotation about an axis with a 340° trend. The gray area is the 95% confidence interval for the inclination-only mean for the measured samples. Modified from figure 94, Shipboard Scientific Party (1995b).

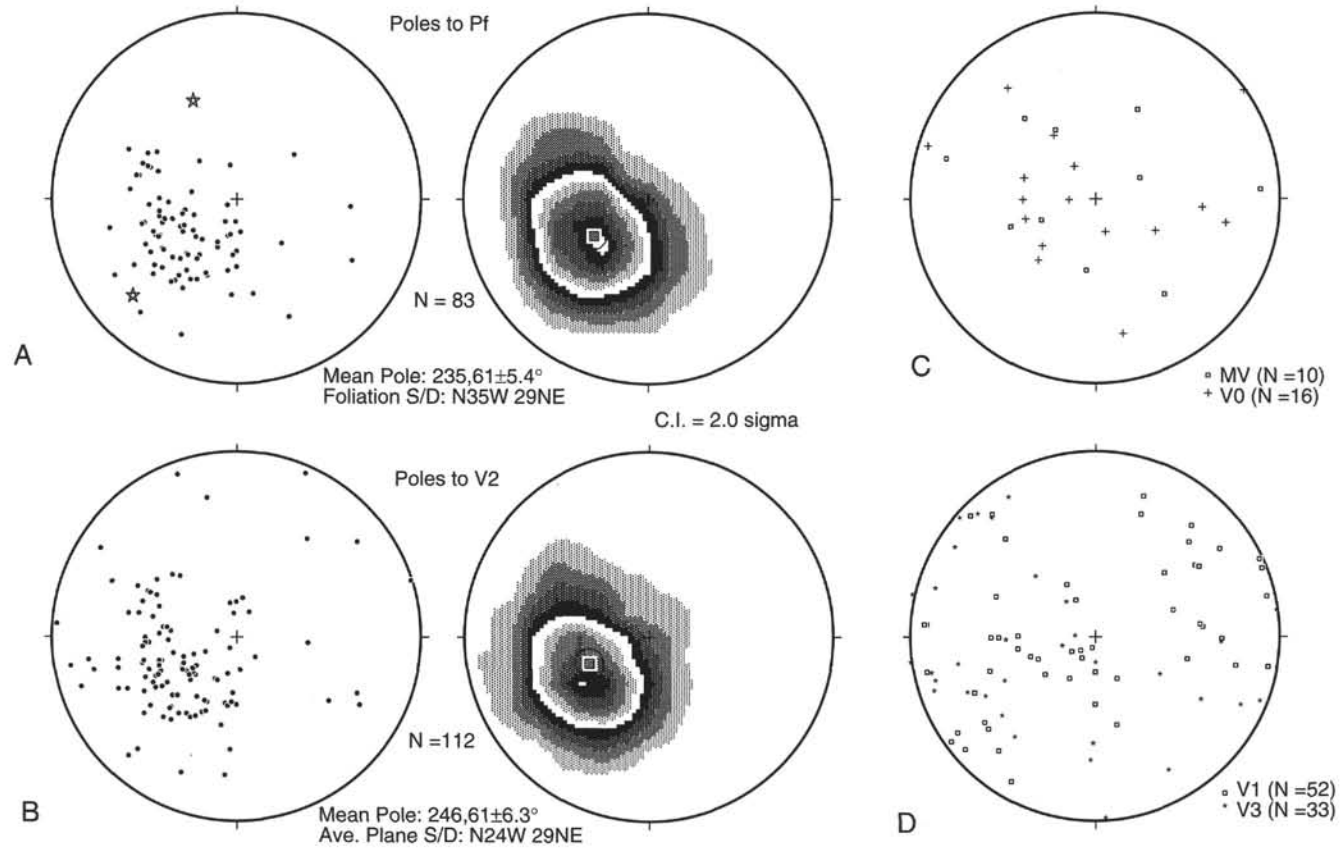

Figure 6. Stereographic projections of the reconstructed orientation of the deformation structures (foliation, veins) in core from Holes 920B and 920D. The measured stable remanent magnetic declination was rotated to due north and orientations of features measured in the core reference frame appropriately restored. Combined measurements for both holes are shown on lower hemisphere equal-area stereographic projections. **A.** Scatter plot of poles to the plastic foliation defined by elongate remnants of orthopyroxene crystals, and accompanying Kamb contour plot. Also shown as stars are the stable remanent magnetic directions for two oriented samples collected by *Alvin* near Site 920. **B.** Equivalent diagrams for the V2 generation of veins. **C.** Combined scatter plot of poles to magmatic veins (MV) and vein set V0. **D.** Combined scatter plot of poles to veins generations V1 and V3. Note that poles to the V3 vein set do not occur in the upper right quadrant, therefore the average V3 vein has a dip to the northeast, similar to the plastic foliation and the V2 vein set.

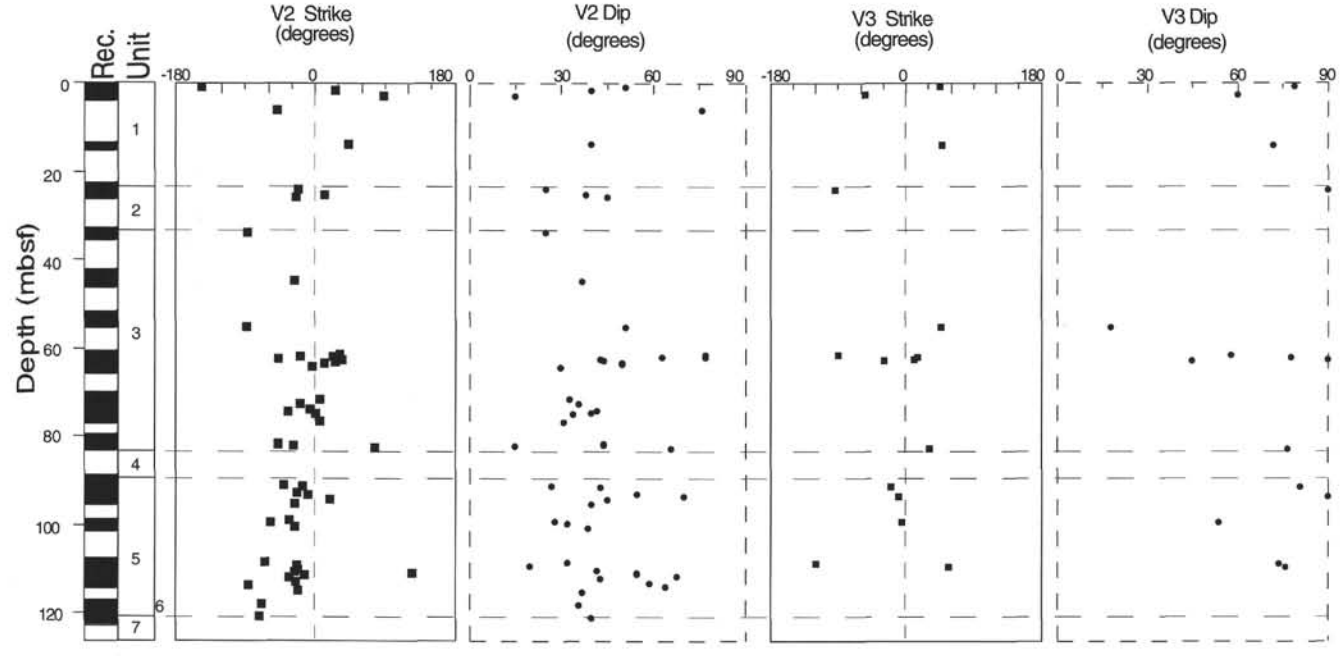

Figure 7. Downhole orientation variations for the V2 and V3 veins sets in Hole 920. The average V2 strike is 343° and the dip is 35°. Note that the orientation of the strike is generally more west trending at the deepest samples. Although the V3 vein set has many fewer corrected orientations measured, the average strike is near 0°, although V3 dips are generally much greater than those for V2 veins. Rec. = recovery.

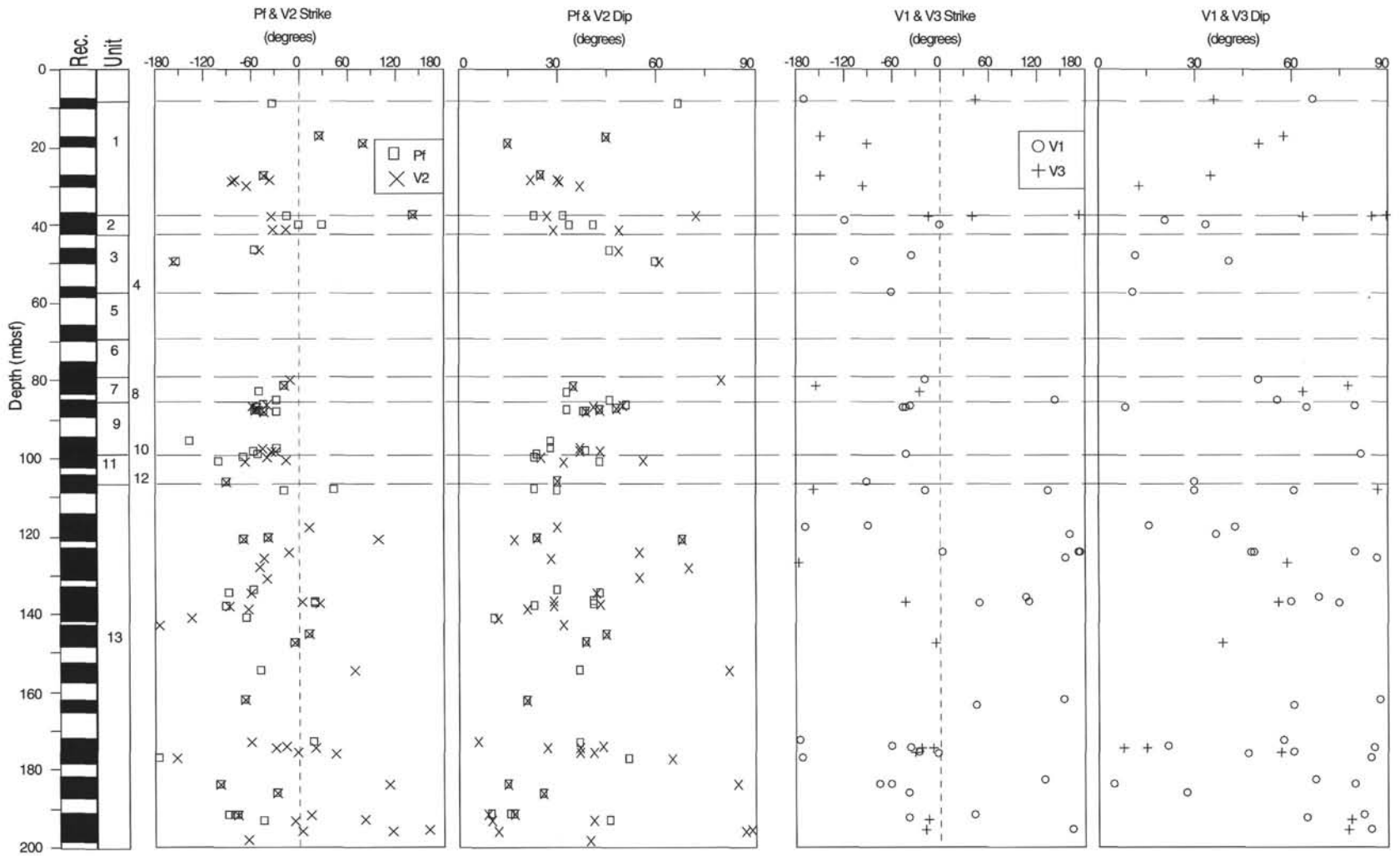

Figure 8. Downhole orientation variations for the plastic fabric (PF) and several vein sets in Hole 920D. The first two columns show strike and dip for PF and V2 combined. In general, these features are parallel, although near the bottom of the hole significant differences in both strike and dip are common. The mean orientation of V2 is N33°W, 25°NE, and of PF is N41°W, 24°NE. The V1 and V3 vein generations show no coherent variation in orientation with depth. Rec. = recovery.

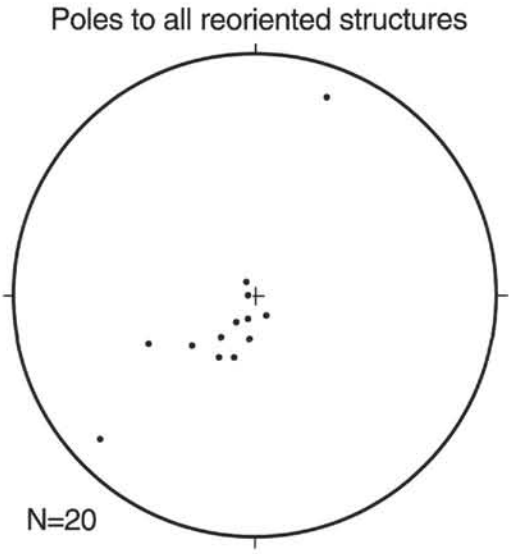

Figure 9. Equal-area stereographic projection of reoriented structures in core from Hole 923A. This hole was drilled to approximately 80 m with very high recovery.

Table 4. Reorientation data for samples from Hole 923A

Core, section	Piece	Char. declin. (°) (uncorr.)	Feature	Strike, dip (°) (uncorr.)	Strike, dip (°) (corr.)
2R-1	4	356	PF	147, 47	151, 47
2R-1	4	356	V	291, 37	295, 37
2R-2	1	18	V5a	347, 39	329, 39
2R-2	1	18	SZ	166, 56	148, 56
2R-2	1	18	V4a	30, 49	12, 49
2R-2	1	18	J	57, 64	39, 64
2R-2	1	18	V4	45, 76	27, 76
2R-2	1	18	V5b	10, 40	352, 40
2R-2	8	162	PF	305, 46	143, 46
2R-2	8	162	MV	225, 59	63, 59
2R-2	8	162	V	159, 16	357, 16
3R-1	3A	90	Va	5, 55	275, 55
3R-1	3A	90	CTV	168, 41	78, 41
3R-1	3A	90	PF	120, 49	30, 49
3R-1	3B	90	V	76, 21	346, 21
3R-1	5A	29	Vc	247, 8	218, 8
3R-1	5A	29	Pf	131, 30	102, 30
3R-1	5A	29	Va	90, 44	61, 44
3R-1	5B	29	CTV	130, 27	101, 27
3R-1	5C	29	BS	180, 15	151, 15
3R-1	6	264	CTV	192, 22	288, 22
3R-1	6	264	CTV	204, 24	300, 24
3R-1	6	264	PF	213, 18	309, 18
3R-1	6	264	CTV	225, 27	321, 27
3R-2	2	54	SZ	206, 45	152, 45
3R-2	2	54	PF	206, 45	152, 45
4R-1	7	84	PF	160, 32	76, 32
4R-1	7	84	Vb	99, 75	15, 75
4R-1	7	84	Va	90, 78	6, 78
5R-2	2	111	Vc	152, 25	41, 25
5R-2	2	111	Vb	147, 37	36, 37
5R-2	2	111	Va	122, 27	11, 27
5R-2	2	111	J	170, 50	59, 50
5R-2	3	188	V	212, 66	24, 66
6R-2	1	274	V	249, 21	335, 21
7R-1	9	194	Va	114, 76	280, 76
7R-1	9	194	MF	340, 9	146, 9
8R-1	5	14	V1	328, 66	314, 66
8R-1	5	14	CL	141, 44	127, 44
8R-3	1	348	PF	174, 18	186, 18
8R-3	1	348	Va	192, 32	204, 32
9R-1	4	75	CTV	221, 32	146, 32
9R-2	8	295	Vb	160, 73	225, 73
9R-2	8	295	CTV	50, 15	115, 15
9R-2	8	295	PF	50, 15	115, 15
9R-2	8	295	Va	325, 12	30, 12
10R-1	5A	269	V4	0, 68	91, 68
10R-1	5A	269	MV	7, 68	98, 68
10R-1	5A	269	V3	326, 75	57, 75
10R-1	5A	269	Pf	57, 14	148, 14
10R-2	1	90	V	30, 32	300, 32
10R-2	2A	8	CTVb	293, 8	285, 8
10R-2	2B	8	CTV	0, 2	352, 2
10R-2	2B	8	PF	247, 8	239, 8
10R-2	2B	8	MF	311, 11	303, 11
11R-1	7	239	CTV	214, 40	335, 40
11R-1	7	239	Bss	214, 40	335, 40
11R-1	7	239	PF	214, 40	335, 40
11R-1	7	239	V	214, 40	335, 40
11R-1	8	23	SZ	1170, 60	147, 60
11R-1	8	23	CTV	183, 30	160, 30
11R-1	8	23	PF	183, 30	160, 30
11R-2	5	8	V	60, 263	52, 26
11R-2	5	8	V	5170, 11	162, 11
12R-1	5	314	IC	0, 54	46, 54
12R-1	5	314	Vd	354, 62	40, 62
12R-1	5	314	Vb	29, 24	75, 24
12R-1	5	314	Vc	19, 40	65, 40
12R-1	5	314	Va	34, 35	80, 35
12R-1	5	314	Vf	333, 70	19, 70
12R-2	1	87	PF	180, 40	93, 40
12R-2	1	87	V	104, 12	17, 12
12R-2	1	87	MVa	214, 40	127, 40
12R-2	1	87	MVb	214, 40	127, 40
12R-2	2	171	MVa	195, 73	24, 73
12R-2	2	171	Va	195, 73	24, 73
12R-2	2	171	Vb	195, 73	24, 73
13R-1	13	226	V4b	188, 53	322, 53
13R-1	13	226	PF	232, 22	6, 22
13R-1	13	226	V4a	108, 25	242, 25
13R-3	2	184	V	141, 76	317, 76
13R-3	6	24	PF1	188, 59	164, 59
13R-3	6	24	PF2	205, 48	181, 48
13R-3	6	24	V	148, 91	24, 9
14R-1	8	55	V	2, 52	307, 52
14R-2	1	157	V	186, 60	29, 60
15R-3	1	151	Vd	335, 58	184, 58
15R-3	1	151	Ve	166, 71	15, 71
15R-3	1	151	Va	33, 29	242, 29
15R-3	1	151	Vc	8, 70	217, 70
15R-3	1	151	Vb	168, 63	17, 63
16R-2	1	178	V2b	255, 11	77, 11
16R-2	1	178	SZ	342, 58	164, 58
16R-2	1	178	V4	90, 90	272, 90
16R-2	1	78	V3	324, 62	146, 62
16R-2	4	41	V4	151, 76	110, 76
16R-3	1	159	V3	217, 5	58, 5
16R-3	5	162	V	198, 24	36, 24
16R-4	7	135	CTV	328, 33	193, 33
16R-4	7	135	F	167, 17	32, 17

Notes: The correction factor is equal to 360° – D (the uncorrected characteristic remanent declination). Therefore the corrected orientations are in the system where north is parallel to the remanent declincation. Abbreviations: BS = brittle shear zone; CL = compositional layering; CTV = composition or textural variation; F = fault; IC = igneous contact; J = joint; MF = magmatic fabric; MV = magmatic vein; SZ = shear zone; PF = plastic fabric; V* = vein with number in the piece. Other abbreviations as in Table 2.